Supplementary Information

Liquid nitrogen driven assembly of nanomaterials into spongy millispheres for various applications

Yimin Yao, [†,‡] *Yunming Li*, [†,‡] *Xiaoliang Zeng,* [*,†] *Na Sun*, [†,//] *Rong Sun,* [*,†] *Jian-Bin Xu*, [*,§] *Ching-Ping Wong*[†,§,⊥]

Contents

- **Fig. S6.** MIP data of silicon carbide nanoparticle-based sphere in intrusion for cycle 1. (A) Cumulative Intrusion vs Pressure, (B) Cumulative Pore Area vs Pore size, (C) Cumulative Intrusion vs Pore size, and (D) Log Differential Intrusion vs Pore size.
- **Fig. S7.** Microstructure of Al_2O_3-based spongy spheres. (A) SEM image of initial Al_2O_3 particles. (B) Digital image of Al_2O_3-based spongy spheres. (C, D) Surface morphology of Al_2O_3-based spongy spheres at different magnifications.
- Movie S1 (.mpg format). Fabrication of GO spongy spheres.
- Movie S2 (.mpg format). Fabrication of silicon carbide nanowire-based spongy spheres.
- Movie S3 (.mpg format). Fabrication of silicon carbide nanoparticle-based spongy spheres.
- Movie S4 (.mpg format). The adsorption capability of BN spheres.

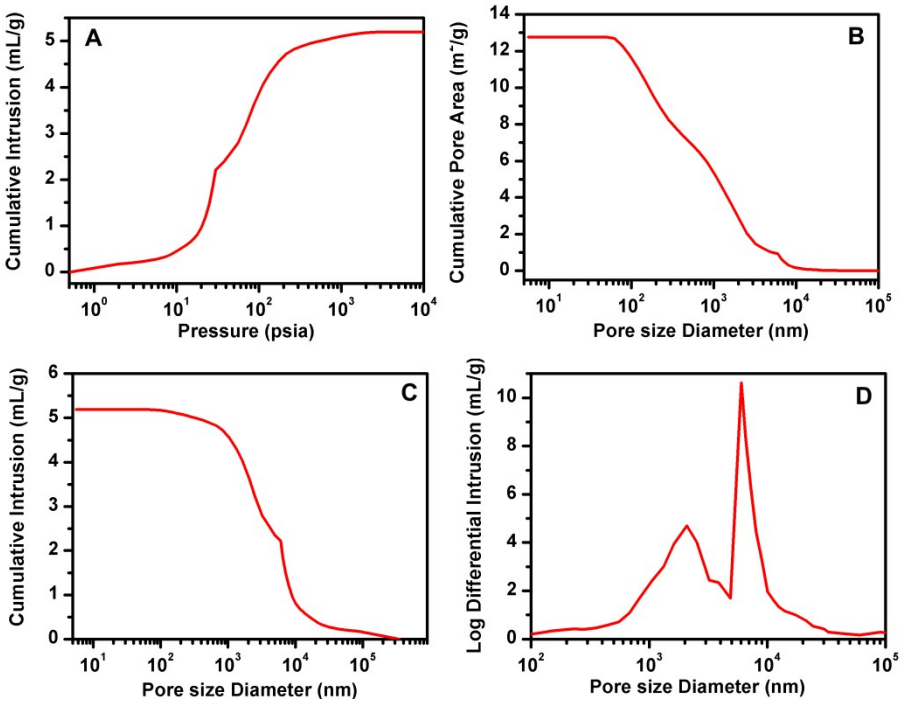

Fig. S1. MIP data of graphene oxide sphere in intrusion for cycle 1. (A) Cumulative Intrusion vs Pressure, (B) Cumulative Pore Area vs Pore size, (C) Cumulative Intrusion vs Pore size, and (D) Log Differential Intrusion vs Pore size.

Median Pore Diameter (Area) = 1074.8 nm

Average Pore Diameter (4V/A) = 3356.1 nm

Porosity = 86.4932 %

BET Surface Area = 221.27 m^2/g

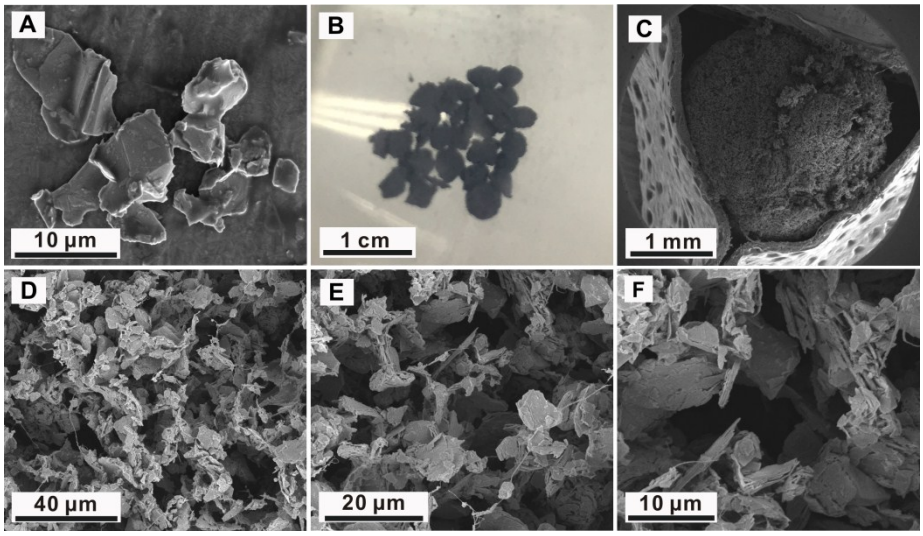

Fig. S2. Microstructure of MoS_2-based spongy spheres. (**A**) SEM image of initial MoS_2 sheets. (B) Digital image of MoS_2-based spongy spheres. (C) SEM image of a single spongy sphere. (D-F) Surface morphology of MoS_2-based spongy spheres at different magnifications.

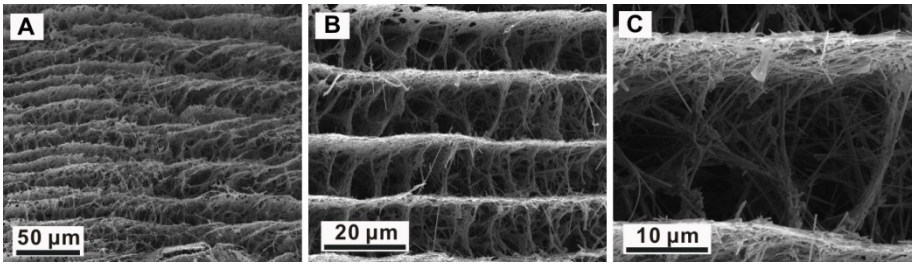

Fig. S3. Microstructure of silicon carbide nanowire-based spongy spheres. (A-C) Surface morphology of silicon carbide nanowire-based spongy sphere (18 $mg \cdot cm^{-3}$) at different magnifications.

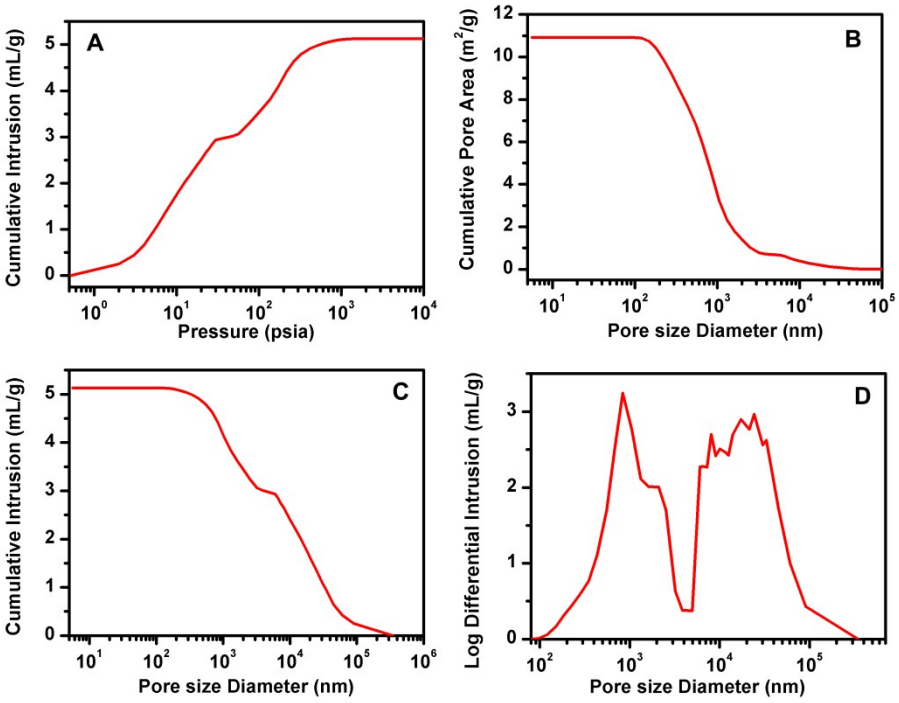

Fig. S4. MIP data of silicon carbide nanowire-based sphere in intrusion for cycle 1. (A) Cumulative Intrusion vs Pressure, (B) Cumulative Pore Area vs Pore size, (C) Cumulative Intrusion vs Pore size, and (D) Log Differential Intrusion vs Pore size.

Median Pore Diameter (Area) = 729.5 nm

Average Pore Diameter (4V/A) = 1979.7 nm

Porosity = 88.2192 %

BET Surface Area = 247.21 m²/g

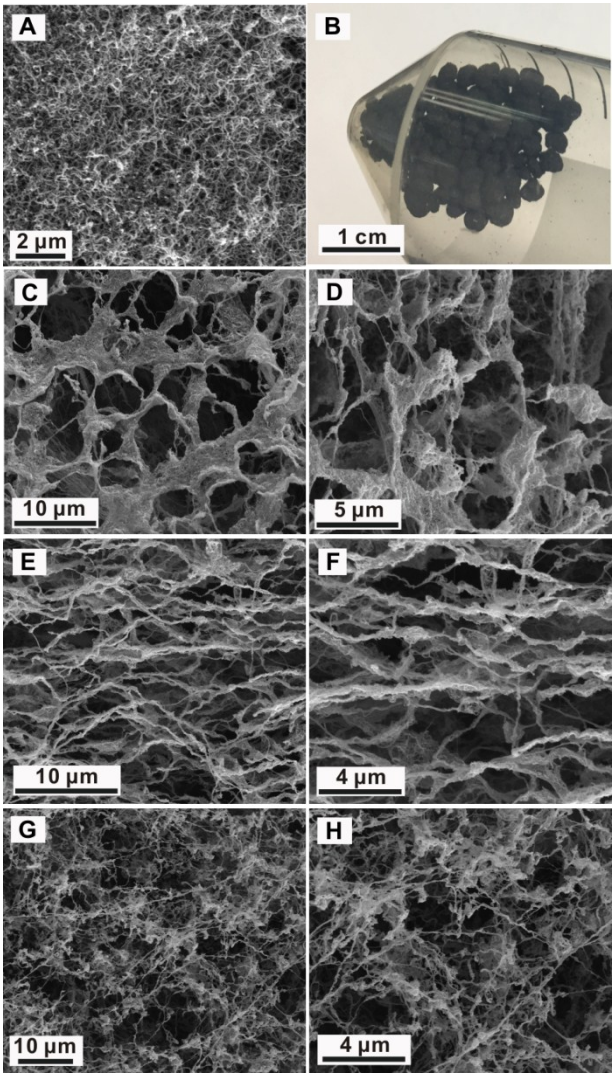

Fig. S5. Microstructure of CNT-based spongy spheres. (A) SEM image of initial CNT. (B) Digital image of the obtained CNT-based spongy spheres. Surface morphology of CNT-based spongy spheres with different densities: (C, D) 25 mg·cm^{-3}, (E, F) 50 mg·cm^{-3}, and (G, H) 75 mg·cm^{-3}.

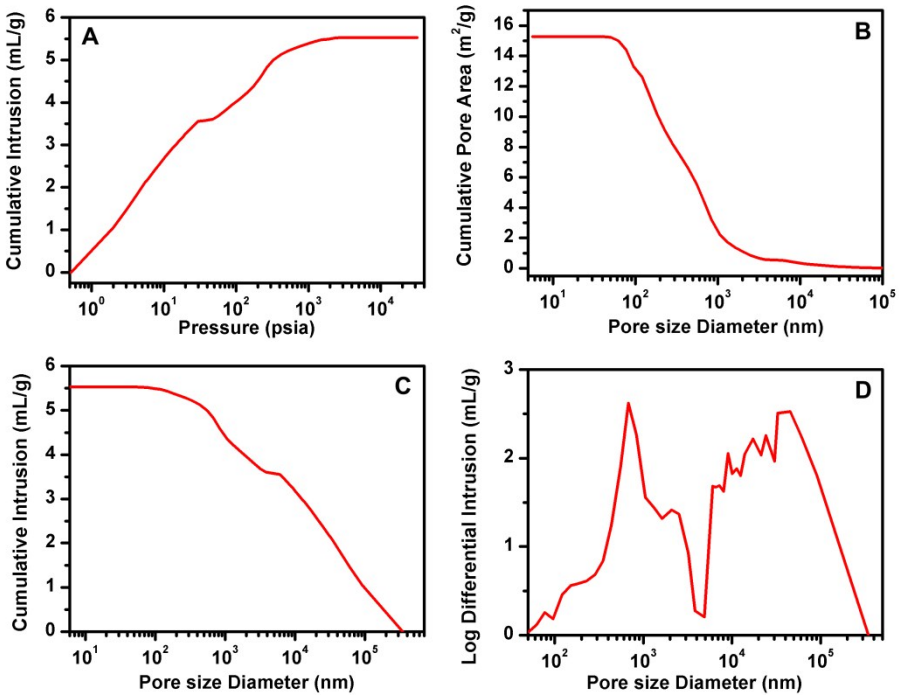

Fig. S6. MIP data of silicon carbide nanowire-based sphere in intrusion for cycle 1. (A) Cumulative Intrusion vs Pressure, (B) Cumulative Pore Area vs Pore size, (C) Cumulative Intrusion vs Pore size, and (D) Log Differential Intrusion vs Pore size.

Median Pore Diameter (Area) = 436.9 nm

Average Pore Diameter (4V/A) = 1548.8 nm

Porosity = 87.8663 %

BET Surface Area = 282.28 m²/g

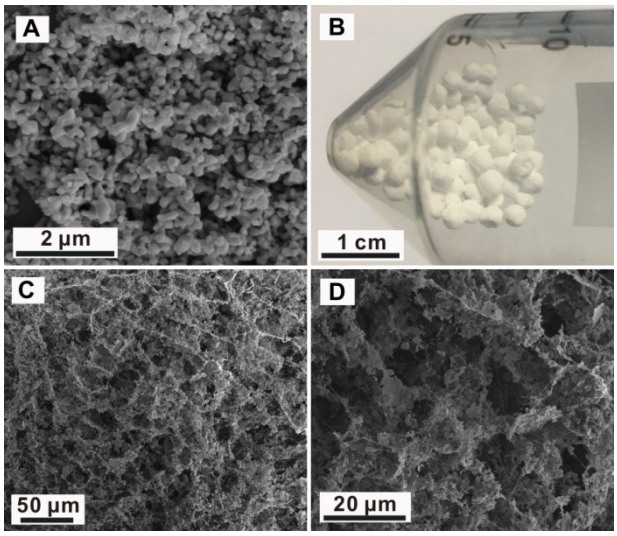

Fig. S7. Microstructure of Al_2O_3-based spongy spheres. (A) SEM image of initial Al_2O_3 particles. (B) Digital image of Al_2O_3-based spongy spheres. (C, D) Surface morphology of Al_2O_3-based spongy spheres at different magnifications.